Generating Shake Maps: Conditional GMPE-based Ground Shaking Fields with Site Effects

Andrea Miano[a], Fatemeh Jalayer[a], Giovanni Forte[b], Antonio Santo[b]
[a] *Università degli Studi di Napoli Federico II, Dipartimento di Strutture per l'Ingegneria e l'Architettura, Via Claudio 21, 80125 Napoli, Italy*
[b] *Università degli Studi di Napoli Federico II, Dipartimento d'Ingegneria Civile, Edile ed Ambientale, Piazzale Tecchio 80, 80125 Napoli, Italy*

Keywords: Shake maps, Ground motion prediction equations, Spatial correlation, Site specific effects

ABSTRACT
Shake maps are useful tools for spatial mapping of the ground shaking for a given earthquake event. They are often used for calculating the empirical fragilities by associating the ground shaking level at a given building's location to the observed damage at that location. Alternatively, the ground shaking can be mapped for a given earthquake event by using the ground motion prediction equations (GMPE's). However, the GMPE's often have a considerable prediction error and they usually do not consider the non-linear stratigraphic effects and the effect of topography. Ground-shaking fields can be generated according to the joint probability distribution of ground-shaking at the locations of interest considering the spatial correlation structure in the ground motion prediction residuals and updated based on the registered ground shaking data. As alternative to the embedded coefficients in the ground motion prediction equations accounting for subsoil categories, site-specific stratigraphic non-linear relationships based on microzonation studies can be applied directly to the ground motion fields at the engineering bed rock level. It is also possible to apply topographic amplification/deamplification factors considering the shape of site slopes. An application of the proposed procedure in generating stochastic ground motion fields for the 2016 Amatrice Earthquake both for a given areal extent and for a class of residential masonry buildings damaged in the central Italy sequence is presented. Regarding the derivation of empirical fragilities, it has been demonstrated that explicit consideration of the spatial correlation in the prediction of ground-shaking fields and the site effects significantly affects the results.

1 INTRODUCTION

Accurate assessment of seismic risk for buildings at a territorial scale depends to a large extent on the availability of reliable procedures to accurately estimate the ground-shaking at the location of these buildings. Shake maps are useful tools for spatial mapping of the ground shaking for a given earthquake event. They are often used for calculating the empirical fragilities by associating the ground shaking level at a given building's location to the observed damage at that location. Alternatively, the ground shaking can be mapped for a given earthquake event by using the ground motion prediction equations (GMPE's). In fact, one important aspect that emerges from the available rich literature on empirical vulnerability and fragility assessment is that accurate estimation of the ground shaking level is crucial (at least as much as accurate damage estimation) towards accurate and reliable empirical fragility assessment. This work revisits a methodology for the generation of conditional GMPE-based ground shaking fields (Park et al. 2007, Crowley et al. 2008, Miano et al. 2015, 2016). The application of this "home-made" shakeMap is demonstrated in generating stochastic ground motion fields for the 2016 Amatrice Earthquake both for a given areal extent and for a class of residential masonry buildings damaged in the central Italy sequence. The basic underlying idea (like the method described in Miano et al. 2016 for portfolio loss assessment) comes from the consideration that the ground shaking levels recorded at adjacent buildings are going to reveal significant spatial correlation. This calls for adopting a full probabilistic model based on the GMPE, where the inter-event and intra-event correlations between the GMPE residuals are characterized (e.g., Park et al. 200; Jayaram and Baker 2009; Goda and Atkinson 2010; Goda 2011; Sokolov and Wenzel 2011). Assuming that

the ground shaking levels registered at different sites are jointly Lognormally distributed, the GMPE's considering a spatial correlation structure are expressed in terms of multivariate Lognormal joint probability distributions. Moreover, the ground shaking propagated to the bed rock level using the GMPE can be modified (or propagated to the surface) based on site-specific stratigraphic and topographic considerations. Alternatively, the ground-shaking can be estimated directly at the surface by employing the coefficients embedded in the GMPE to take into account the site conditions. Then, a "complete" GMPE representation through the joint Lognormal probability distribution can be updated both based on the recorded registrations of the earthquake event of interest at the surrounding stations (e.g, Park et al. 2007, Crowley et al. 2008, Miano et al. 2015, 2016) and the observed damage pattern. Finally, an alternative shakeMap can be generated as stochastic realizations of the ground shaking field according to the updated GMPE description at the ground surface. In this work, an application of the proposed "home-made" shakeMap is presented for generating stochastic ground motion fields for the 2016 Amatrice Earthquake both for a given areal extent and for a class of residential masonry buildings damaged in the central Italy sequence. Regarding the derivation of empirical fragilities, it has been demonstrated that explicit consideration of the spatial correlation in the prediction of ground-shaking fields and the site effects significantly affects the results.

2 METHODOLOGY FOR GENERATION OF SCENARIO- AND GMPE-BASED GROUND SHAKING FIELDS

*2.1 Generation of scenario- and GMPE-based ground shaking fields based on f(**PGA**)*

The joint probability density function *f*(**PGA**) for the vector of **PGA**=[PGA_i, i=1:N_{cl}] values at the location of each site of interest for a given earthquake scenario can be evaluated by employing a ground motion prediction equation (GMPE). A full probabilistic representation (based on the first two moments) of GMPE can be expressed in terms of multivariate Normal distribution which is identified by its expected value vector **M** and covariance matrix **Σ**. That is, once the first two moments and are given, several realizations of the ground shaking field can be generated.

Herein, the model proposed by Bindi et al. (2011, **ITA10**) for the peak ground acceleration (PGA, the geometric mean of two horizontal components) as the intensity measure is used. The functional form of this model is the following:

$$\mathrm{E}[\log_{10}\mathrm{PGA}] = e_1 + F_D\left(R_{jb}, M\right) + \\ +F_M\left(M\right) + F_S + F_{sof} \quad (1)$$

where E[$\log_{10}$PGA] is the expected value (first moment) for the (base 10) logarithm of peak ground acceleration (PGA, in cm⁄s^2); e_1 is a constant term, F_D (R_{jb},M), F_M(M), F_s and F_{sof} represent the distance function, the magnitude scaling, the site amplification and the style of faulting correction, respectively. M is the moment magnitude, R_{jb} is the Joyner–Boore distance in km (or the epicentral distance when the fault geometry is unknown --generally when M<5.5). The proposed equation for the distance function F_D (R_{jb},M) is:

$$F_D\left(R,M\right) = \left[c_1 + c_2 \cdot \left(M - M_{ref}\right)\right] \cdot \\ \log_{10}\left(\sqrt{R_{jB}^2 + h^2 / R_{ref}}\right) - c_3 \cdot \left(\sqrt{R_{jB}^2 + h^2 / R_{ref}}\right) \quad (2)$$

the magnitude function F_M(M) is expressed as:

$$F_M\left(M\right) = b_1 \cdot \left(M - M_h\right) + \\ +b_2 \cdot \left(M - M_h\right)^2 \quad if \quad M \le M_h \quad (3)$$

$$F_M\left(M\right) = b_3 \cdot \left(M - M_h\right) \quad if \quad M > M_h \quad (4)$$

where M_{ref}, M_h, and R_{ref} are fixed as R_{ref}=1km, M_{ref}=5, M_h=6.75. The functional form F_S in Eq.3 represents the site amplification and it is given by F_S=s_jC_j, for j=1:5, where s_j are site amplification coefficients provided by Bindi et al. (2011) and C_j are dummy binary variables corresponding to the five different EC8 site classes. Finally, the functional form F_{sof} represents the faulting correction coefficient and it is given by F_{sof} =f_jE_j, for j=1:4, where fj are style of faulting coefficients and E_j are dummy binary variables used for the different faulting styles (i.e., normal (*N*), reverse (*R*), strike slip (*SS*) and unknown (*U*)). The values E[$\log_{10}$PGA$_i$] (i=1:N_{cl}) from Eq. (3) constitute the components of the mean vector **M**. The covariance matrix, **Σ**, is defined as the sum of two inter-event and intra-event components:

$$\mathbf{\Sigma} = \sigma_{INTER}^2 \cdot \mathbf{e} + \sigma_{INTRA}^2 \cdot \mathbf{R} \quad (5)$$

where σ_{intra} represents the intra-event variability and σ_{inter} represents the inter-event variability (both parameters are tabulated in Bindi et al. 2011); **e** is the all ones matrix and **R** is the matrix of correlation coefficients. **R** is composed of unit diagonal terms and off-diagonals equal to

ρ_{jk}, $j \neq k$ (both varying from 1 to N_{cl}; where N_{cl} is the number of buildings surveyed for building class *CL*). The covariance matrix is obtained according to the following formulation of ρ_{jk} (Esposito and Iervolino, 2012):

$$\rho_{jk} = \exp\left[-3 \cdot h_{jk} / b(T)\right] \quad (6)$$

where h_{jk} represents the distance between sites j and k and $b(T)$ is a coefficient set equal to 10.8km. It is to note that the above expression for the correlation coefficient has been calibrated to the residuals of the Bindi et al. (2011) GMPE adopted herein and therefore is reasonably consistent for the purpose used in this study.

2.2 Considering stratigraphic and topographic factors

As mentioned in the previous section, the GMPE adopted herein considers the site effects as a function of V_{s30}-dependent European Code soil classifications. Nevertheless, in order to consider as accurately as possible the site effects, it is important to incorporate the results of more sophisticated seismic microzonation studies for the surveyed buildings sites. For example, Landolfi et al. (2011) and later Tropeano et al. (2018) propose site-specific stratigraphic coefficients that consider non-linear soil column propagation effects. Herein, two alternatives are considered for taking into account the stratigraphic site effects; namely, (a) the coefficients imbedded in the GMPE (here Bindi et al. 2011, **ITA10**); (b) application of stratigraphic amplification factors to ground shaking at bedrock (e.g., those reported in Landolfi et al. 2011). Landolfi et al. (2011) have merged empirical, semi-empirical and analytical datasets to compute non-linear relationships quantifying stratigraphic amplification for different classes of subsoil profiles. That is, site effects are evaluated through the stratigraphic amplification factor, which is directly multiplied by the reference (i.e., propagated to bed-rock) peak ground acceleration from the GMPE by Bindi et al. (2011) to obtain the peak acceleration at surface:

$$\begin{aligned} S_B &= 1.028 \cdot PGA_r^{-0.15}; \sigma = \pm 0.099 \\ S_C &= 1.028 \cdot PGA_r^{-0.23}; \sigma = \pm 0.098 \\ S_D &= 1.028 \cdot PGA_r^{-0.42}; \sigma = \pm 0.136 \end{aligned} \quad (7)$$

Moreover, it is also possible to apply topographic amplification/deamplification factors (S_T) to the GMPE. S_T depends on the shape of slopes, since irregular surface geometry affects the focusing, defocusing, diffraction and scattering of seismic waves. This can lead to a change in amplitude, frequency and duration of ground motion compared to flat ground conditions (Paolucci, 2002). Following Garcìa–Rodriguéz et al. (2008), a geometrical parameter more suitable for small scale studies seemed to be the slope curvature, which can be obtained from the DEM of the area. This index permits to mark the concave and the convex features of a landscape, with negative and positive values respectively, accounting for attenuation in valleys and the seismic waves focusing on ridges. The effectiveness of this parameter was also validated by the numerical study of Torgoev et al. (2013) and adopted in seismic slope stability analyses by Silvestri et al. (2016) and reported in Table 1.

Table 1. Curvature (α') ranges and associated S_T.

Curvature (α')	S_T	Class
< -0.5	0.6	1
-0.5 ÷ -0.2	0.8	2
-0.2 ÷ 0.2	1	3
0.2 ÷ -0.5	1.2	4
> 0.5	1.4	5

It should be noted that the above-mentioned stratigraphic and topographic factors are going to be applied herein in a deterministic manner. It can be shown that this changes the mean vector **M** through an additive constant (i.e., the inner product of a vector of constant factors by the median in the arithmetic scale) and leaves the covariance matrix **Σ** un-altered.

*2.3 Updating the generated ground shaking fields based on registered PGA data: f(**PGA**|**D**$_{PGA}$)*

One interesting feature of the method adopted herein for generating the ground shaking field realizations is that it can be updated based on the registered values. Recalling from Section 2.3.1, it was assumed that the PGA values at the location of each surveyed building are distributed as a joint multivariate Log (Normal) distribution. One of the specific characteristics of a joint Normal distribution for a vector of variables is that any given partition of the vector conditioned on the remaining components of the vector is still going to be a joint Normal distribution. With specific reference to the case of the vector of $\log_{10}$**PGA** values denoted as data **D**$_{PGA}$, let the vector of mean values M and the covariance matrix **Σ** be partitioned as follows (Park et al. 2007):

$$\mathbf{M} = \begin{bmatrix} \mathbf{M}_1 \\ \mathbf{M}_2 \end{bmatrix} \qquad \mathbf{\Sigma} = \begin{bmatrix} \mathbf{\Sigma}_{11} & \mathbf{\Sigma}_{12} \\ \mathbf{\Sigma}_{21} & \mathbf{\Sigma}_{22} \end{bmatrix} \quad (8)$$

where $\mathbf{M_1}$ is the mean (of the base 10 logarithm) vector of $\mathbf{PGA}=[PGA_i, i=1:N_{cl}]$ values according to the adopted GMPE; $\mathbf{M_2}$ is the mean vector of calculated $\log_{10}$PGA at the stations within the area of interest (according to the adopted GMPE); $\mathbf{\Sigma_{11}}$ is the covariance matrix for the calculated (from the GMPE) $\log_{10}$PGA for the surveyed buildings of class *CL*; $\mathbf{\Sigma_{12}}=\mathbf{\Sigma_{21}}$ is the cross-covariance matrix for the $\log_{10}$PGA values calculated (from the GMPE) at the location of the surveyed buildings and those calculated at the location of the stations; $\mathbf{\Sigma_{22}}$ is the covariance matrix for the $\log_{10}$PGA values calculated at the stations.

As described briefly above, the conditional distribution of the calculated $\log_{10}$PGA values given the registered $\log_{10}$PGA values at the stations is a joint Normal distribution with mean vector $\mathbf{M_{1|2}}$ and covariance matrix $\mathbf{\Sigma_{11|22}}$:

$$\mathbf{M}_{1|2} = \mathbf{M}_1 + \sum_{12} \cdot \sum_{22}^{-1} \cdot \left(\mathbf{D}_{\mathbf{PGA}} - \mathbf{M}_2 \right) \quad (9)$$

$$\sum_{11|22} = \sum_{11} - \sum_{12} \cdot \sum_{22}^{-1} \cdot \sum_{21} \quad (10)$$

where $\mathbf{D}_{PGA}$ is the vector of the registered $\log_{10}$PGA values for the stations. Note that $\mathbf{M_{1|2}}$ and $\mathbf{\Sigma_{11|22}}$ represent the first two moments of the updated joint Lognormal pdf $f(\mathbf{PGA}|\mathbf{D}_{PGA})$.

2.4 Further updating of the generated ground shaking fields based on observed damage D_{cl}: $f(PGA|D_{PGA}, D_{cl})$

One important aspect to highlight is that once the first two moments of the updated ground shaking field corresponding to the Lognormal PDF $f(PGA|D_{PGA})$ are obtained, various plausible realizations of the ground-shaking field can be generated. In this context it is to note that the ground-shaking field is also conditioned on the damage survey data for a given building class. This conditioning is implemented herein based on the premise that only those plausible ground-shaking fields that lead to physically meaningful fragility data are considered. That is, in a rejection sampling logic, those realizations of ground-shaking field which lead to unmeaningful empirical fragility curves are not considered -- assuming that the damage survey is carried out with no error. Finally, it can be argued that the "complete" GMPE representation through the joint Lognormal probability distribution is updated not only based on the recorded registrations of the earthquake event of interest at the surrounding, but also based on the observed damage pattern.

3 APPLICATION

3.1 The study area

Between August and October 2016, Central Italy was stricken by three damaging earthquakes. The first Mw 6.0 event occurred on August 24th at 01:36 UTC close to Accumoli village (herein referred to as Amatrice Earthquake); it was followed by a long seismic sequence, which two months later produced a Mw 5.9 aftershock on October 26th at 19:18 UTC at 3 km West of Visso and a Mw 6.5 event on October 30th at 06:40 UTC, 6 km North of Norcia (see Ebrahimian and Jalayer 2018 for more details about the Central Italy seismic sequence; see Sextos et al. 2018 for more details about observed damage).

The seismic sequence originated in the central Apennine chain on a NW-SE trending normal fault, a typical extensional tectonic regime ongoing since the Late Pliocene (Tinti et al. 2016; Galadini and Galli, 2000). In particular, the 24th August event known as Amatrice earthquake and its aftershocks occurred in the sector between two important regional fault systems, the Laga Mountains (Mts) and Mt. Vettore normal faults. The former affects the base of the western slope of the Laga Mts a ~26 km-long fault-scarp carved onto clayey-arenaceous Miocene flysch, while the Mt. Vettore fault, NW-SE to NNW-SSE trending, is carved onto Meso-Cenozoic limestones (Falcucci et al., 2016). Furthermore, the Central Italy sequence is located in an area bounded to recent earthquakes, in the North by the 1997 Colfiorito and to the South by the 2009 L'Aquila earthquakes (Michele et al., 2016).

This paper focuses on 3 municipalities and 4 fractions; namely, Amatrice, Accumoli, Arquata del Tronto, Tina (Accumuli), Illica (Accumuli), and Pescara del Tronto (Arquata del Tronto),Trisungo (Arquata del Tronto), affected by the 24th August 2016 event as shown in Figure 1. The figure shows a simplified geological map of the area of interest, overlaid with the PGA contour map provided by INGV (Italian Institute of Geophysics and Volcanology) official shakemaps and the fault projection. The area is made of Cenozoic limestones in contact with arenaceous flysch formations through tectonic contacts. The main river valleys are filled with coarse alluvial deposits (gravels and sands), while finer alluvial deposits (silts and clays) manifest themselves in places where paleo-lakes or marshes are present. In certain areas, small outcrops of travertines can also be found.

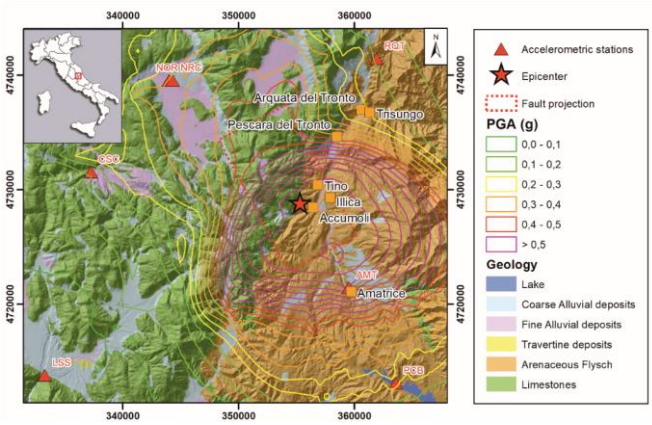

Figure 1: Simplified geologic map of the study area with the PGA distribution of the 24th August 2016 earthquake (INGV ShakeMap).

According to the PGA distribution provided by INGV, ground acceleration values as high as 0.5g affected several small towns in the vicinity of the epicentre. Among these towns, Amatrice is the one that has had the most widespread destruction and the highest number of fatalities. The two hamlets of Tino and Illica have been considered as examples of the stratigraphic and the topographic amplification of ground motion. The masonry buildings located in the above-mentioned towns were strongly damaged by the August 24th event and its aftershocks.

3.2 Damage and vulnerability class identification for the surveyed buildings

The identification of the damage level and of the vulnerability class for the set of buildings used as case study in the next sections is presented in detail in (Miano et al. 2019a and b). However, it is to note that the European Macroseismic Scale EMS 1998 (Grünthal 1998) classification is used in order to identify the damage to the portfolio of masonry buildings considered. The grades of damage are described as follows: Grade 1 (D1): Negligible to slight damage; Grade 2 (D2): Moderate damage; Grade 3 (D3): Substantial to heavy damage; Grade 4 (D4): Very heavy damage; Grade 5 (D5): Destruction. Moreover, it is to consider that the portfolio of surveyed buildings is limited to residential masonry buildings. However, the building inventory can influence the damage scenario (Polese et al. 2019). Four distinct classes of masonry buildings have been defined (Rota et al. 2008): 1) Masonry buildings without tie rods or tie beams with number of stories ≤2 (Masonry Buildings Class 1, MBC1); 2) Masonry buildings without tie rods or tie beams with number of stories >2 (Masonry Buildings Class 2, MBC2); 3) Masonry buildings with tie rods or tie beams with number of stories ≤2 (Masonry Buildings Class 3, MBC3); 4) Masonry buildings with tie rods or tie beams with number of stories >2 (Masonry Buildings Class 4, MBC4).

3.3 Site effects for the surveyed buildings

Post-earthquake field recognition identified, as the most affected area, the valley of Tronto river. This valley is host to several municipalities and hamlets. The local geological and geomorphological setting can be as sketched as shown in Figure 2. Indeed, the villages occupy either the valley close to the river (e.g., Trisungo) or the cliffs overlooking it; with the latter being located usually at the top of small ridges and ancient erosional terraces (e.g. Amatrice, Accumoli, Arquata del Tronto, Figure 2a) or located on the slopes (e.g. Pescara del Tronto, Illica, Tino, Figure 2b).

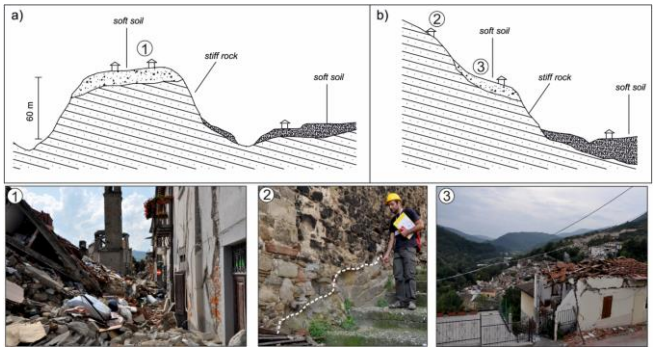

Figure 2: Simplified geological and geomorphological sketch for a) cliff-type; and b) slope-type morphology. 1) Amatrice; 2) Accumoli; 3) Pescara del Tronto.

The villages located on cliff-type morphology (Figure 2a) are almost always bordered by steep slopes (25° - 35°) with heights varying from 20 to 80 m. For these areas, buildings labelled with D4 and D5 damage grades are widespread and mainly localized near the steep escarpments and in the narrower part of the ridges (e.g. Accumuli and Arquata del Tronto). These buildings were affected by seismic waves' focalization due to topographic shape effects (e.g., Grelle et al., 2018). These topographic effects were not present in lowland areas of the valley which suffered less damage, relatively speaking (see Trisungo). On the other hand, other towns (Amatrice, Pescara del Tronto, Illica and Tino), suffered widespread damage due to both topographic and stratigraphic effects (see Figure 2 part 3). Some of these towns lie on slopes characterized by few meters of soft soils resting on a stiffer material (see Figure 2b, Accumuli); where stiff arenaceous formation of the Laga Flysch is buried by few meters of

weathered deposits and colluvium mainly made of silty sands. In the case of Pescara del Tronto, the hamlet lies on debris and travertine sands resting above a limestone bedrock. Figure 3 shows the overall damage break-down with respect to geologic units for MBC 1-4, respectively. It can be observed that, for both structural types, the higher damage grades can be related to a certain degree of stratigraphic amplification (the buildings belonging to damage levels D0 and D1, according to Copernicus EMS 98 scale are grouped with label D1 in Figure 3). For instance, D1 is more frequent on stiff rock such as the Arenaceous flysch and limestones, as shown in Figure 2 (part 2); while D5 is more frequent on coarse alluvial deposits, as they are constituted of soft soil.

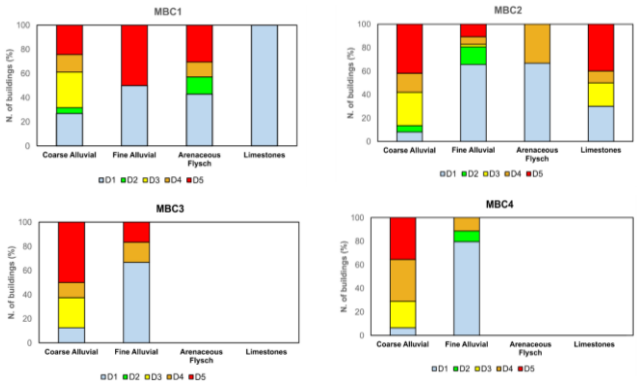

Figure 3: Overall damage break-down with respect to geologic units (source: Copernicus).

In order to account for stratigraphic amplification effects at a small scale, Eurocode 8 seismic soil classes are attributed to the lithological units shown in Figure 3. The attribution (see Table 2) is carried out following the suggestions provided by Forte et al. (2017) for a comparable geo-lithological setting.

Table 2 Seismic Soil class attribution.

Geologic Unit	Geolithological complex (Forte et al., 2017)	EC8 Soil Class
Coarse Alluvial Deposits	CA	B
Fine Alluvial Deposits	FA	B
Travertine	-	B
Arenaceous Flysch	MS	B
Limestone	C	A

3.4 Generation of GMPE-based ground-shaking fields for the Central Italy Earthquake (24 August 2016) scenario

According to the proposed procedure, Nsim=25000 realizations of the GMPE-based ground shaking fields are generated for the Amatrice Earthquake scenario (M=6.0) providing the peak ground acceleration (PGA) for engineering bedrock site conditions. It is worth noting that the realizations are generated for each building class separately. That is, the portfolio of interest is interpreted as the buildings that are attributed to a specific class. In the next step, the generated ground-shaking fields on bedrock are multiplied by the stratigraphic and topographic amplification/deamplification factors calculated according to Equation 7 and Table 1, respectively. Since the uncertainty in the evaluation of these amplification factors is not considered, their application affects only the median M (summed by a constant amplification factors) and leaves the covariance matrix Σ unaffected. Then, in order to obtain the conditional GMPE-based fields, PGA registrations for eighty one accelerometric stations (shown in Figure 4) are employed in order to update the ground motion fields according to the procedure previously described.

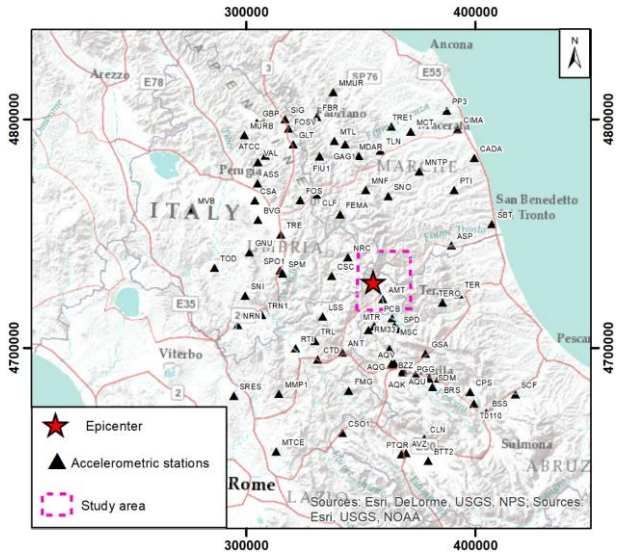

Figure 4: Position of the eighty one accelerometric stations considered in this work.

Figure 5 shows the 16th, median and 84th percentiles modified Bindi GMPE curves for the Amatrice 2016 event (M_w=6.0) and the PGA values recorded by the 81 accelerometric stations, for soil type B and topographic class 3. The 16th, median and 84th percentiles are shown before and after the updating with the registered values from the eighty one accelerometric station. It can be observed, that the median GMPE slightly under-estimates the PGA values for these stations. It can be seen that the recorded values are slightly above the median curve of the Bindi et al. (2011) GMPE.

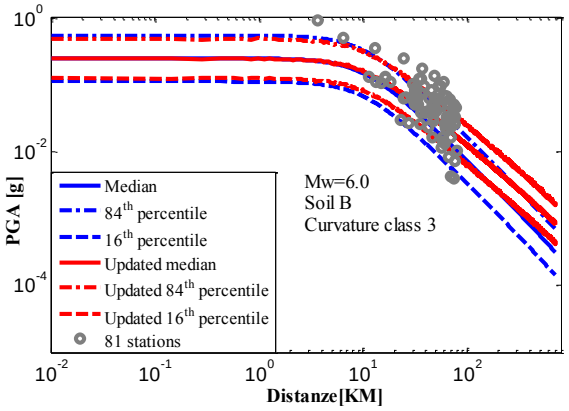

Figure 5: The 16th, median, and 84th percentiles of the GMPE (Bindi et al. 2011), considering the stratigraphic (soil B, Landolfi and Silvestri) and topographic (curvature class 3, Forte and Silvestri) factors applied to the GMPE, before and after the updating with the 81 available registrations.

Figure 6 maps the median PGA values for the Nsim=25000 realizations rendered by a mesh-grid of 500mx500m resolution. Figure 7, instead, demonstrates the median of the conditional GMPE-based ground-shaking field for the surveyed buildings in Amatrice (the largest of the seven towns considered).

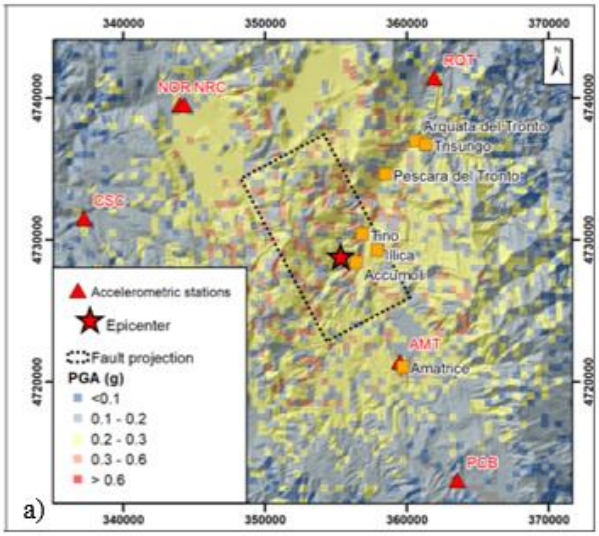

Figure 6: Median of the conditional GMPE-based ground-shaking fields for the Amatrice Earthquake scenario.

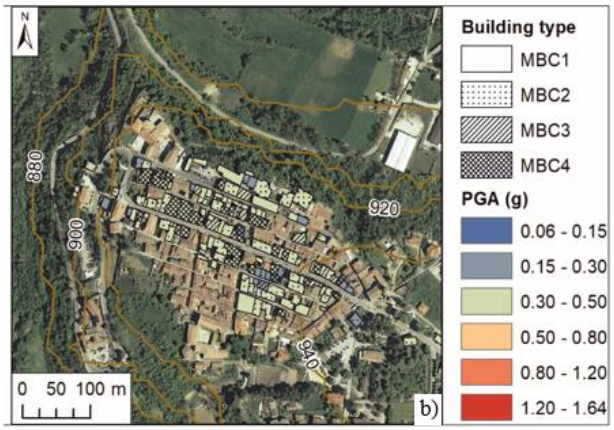

Figure 7: Median of conditional GMPE-based ground-shaking fields for the surveyed buildings in Amatrice.

3.5 Implementation of conditional GMPE-based ground shaking fields with site effects for deriving empirical fragility curves

The empirical fragility assessment herein is performed within an updated robust reliability assessment framework (Jalayer et al. 2010 and 2017, Miano et al. 2019b). The empirical fragility curves have been calculated according to a logistic regression probability model (see e.g. Jalayer and Ebrahimian 2017, Jalayer et al. 2017, De Risi et al. 2017, Miano et al. 2017 and 2018). This type of regression is suitable for cases where the dependent variable is binary (i.e., either 0 or 1). Thus, it is especially suitable for estimating the probability of exceeding a damage state D_i. That is, with regard to damage state D_i, each surveyed building can either: a) exceed the designated damage state denoted as 1 or b) NOT exceed the designated damage state, denoted as 0. Denoting probability of exceeding damage state D_i as a function of the ground-shaking level PGA=x as $\pi i(x)$, the likelihood of having ri buildings that exceed damage state D_i for the N_{CL} buildings surveyed for class CL can be expressed assuming a Binomial Distribution, as described in detail in Miano et al. 2019b. As examples, Figure 8 shows a comparison for masonry class MBC3-D4 between the fragility curves obtained based on the proposed "home-made" shakeMap and the fragility curves obtained based on the INGV shakeMap. The damages grades are based on EMS98 and have been obtained based on both Copernicus-EMS damage grading maps and based on visual survey (Castagna 2017 and Miano et al. 2019b). For all the fragility curves, see Miano et al. 2019a and b. The remarkable different between the two-sets of fragility curves, provides evidence for the sensitivity of the empirical fragility curves to the methods used for the estimation of ground shaking level. Figure 9

shows the empirical fragility curves for masonry buildings MBC2 and damage levels D5 obtained according to Copernicus-EMS damage grading maps (Dcl) the ground shaking fields PGA which consider the effects of stratigraphic amplification as in Bindi et al. (2011) GMPE and as proposed in Landolfi et al. (2011) model. In this second case, Bindi et al. (2011, ITA10) attenuation law is used to propagate the ground-shaking up to bed rock and the coefficients provided in Landolfi et al. (2011) are used to consider the stratigraphic amplification. The comparison shows that the use of Landolfi et al. model is going to slightly reduce both the median and standard deviation with respect to Bindi et al. model. This effect has been observed with varying degrees for all the four building classes considered.

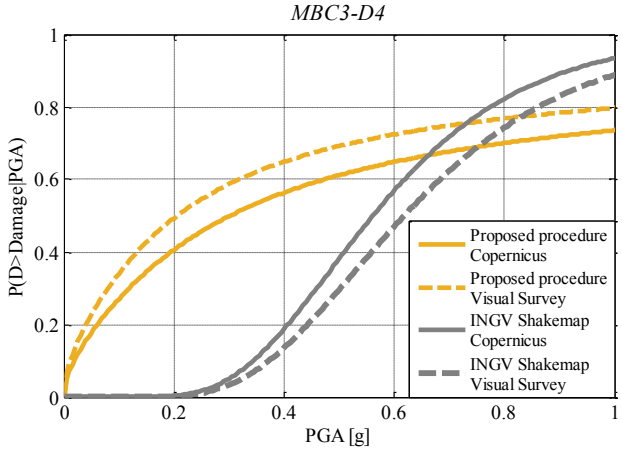

Figure 8: Comparison between the empirical fragility curves for MBC3-D4, obtained based on the proposed "home-made" shakeMap and on the INGV shakemap (damage data from Copernicus-EMS and visual survey).

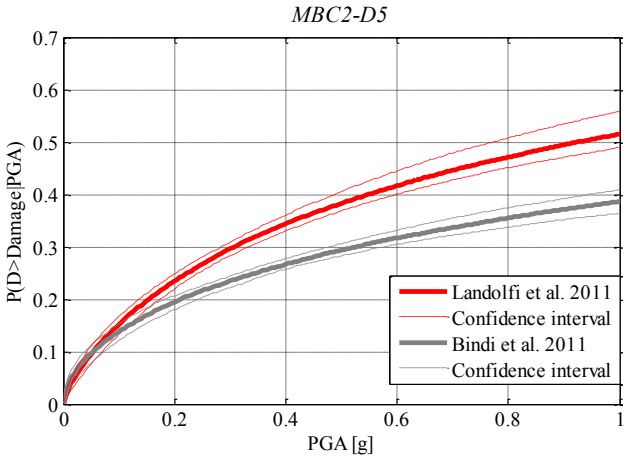

Figure 9: Comparison between the fragility curves obtained using the stratigraphic coefficients from Bindi et al. (2011) and from Landolfi et al. (2011) for masonry building class MBC2 and damage levels D5.

4 CONCLUSIONS

Shake maps are useful tools for spatial mapping of the ground shaking for a given earthquake event. Alternatively, the ground shaking can be mapped for a given earthquake event by using the GMPE's. However, the GMPE's often have a considerable prediction error and they usually do not consider the non-linear stratigraphic effects and the effect of topography. Ground-shaking fields can be generated according to the joint probability distribution of ground-shaking at the locations of interest considering the spatial correlation structure in the ground motion prediction residuals and updated based on the registered ground shaking data. Moreover, it is also possible to consider site specific stratigraphic and topographic factors. An application of the proposed procedure in generating stochastic ground motion fields for the 2016 Amatrice Earthquake both for a given areal extent and for a class of residential masonry buildings damaged in the central Italy sequence is presented. Implementation of the proposed procedure for deriving empirical fragilities is discussed. It has been demonstrated that explicit consideration of the spatial correlation in the prediction of ground-shaking fields and the site effects significantly affects the results. In fact, the fragility curves obtained based on INGV shakeMap and those obtained by following the proposed procedure demonstrate differences for all the classes. Generally speaking, for the specific case-study, the empirical fragility curves obtained based on the proposed procedure demonstrate smaller median and larger dispersion with respect to those obtained based on the shakeMap. Furthermore, specific consideration of the nonlinear stratigraphic effect and the effect of topography affects to varying degrees the resulting empirical fragility curves. This provides evidence for the remarkable sensitivity of the empirical fragility curves to the methods used for the estimation of ground shaking level.

ACKNOWLEDGEMENTS

This work is based on visual damage survey results described in the B.Sc. thesis of Filomena Castagna. This support is gratefully acknowledged.

REFERENCES

Bindi, D., Pacor, F., Luzi, L., Puglia, R., Massa, M., Ameri, G., Paolucci, R., 2011. Ground motion prediction equations derived from the Italian strong motion

database. *Bulletin of Earthquake Engineering*, **9**(6),1899–1920.

Castagna, F., 2017. La valutazione della vulnerabilità sismica degli edifici danneggiati a seguito del terremoto di Amatrice del 24 agosto 2016. B.Sc. in Civil Engineering, University of Naples Federico II.

Crowley, H., Bommer, J.J., Stafford, P.J., 2008. Recent developments in the treatment of ground-motion variability in earthquake loss models. *Journal of Earthquake Engineering*, **12**(S2):71–80.

De Risi, R., Jalayer, F., De Paola, F., Lindley, S., 2017. Delineation of flooding risk hotspots based on digital elevation model, calculated and historical flooding extents: the case of Ouagadougou. *Stochastic environmental research and risk assessment*, 1-15.

Ebrahimian, H., Jalayer, F., 2017. Robust seismicity forecasting based on Bayesian parameter estimation for epidemiological spatio-temporal aftershock clustering models. *Scientific reports* **7**(1), 9803.

Esposito, S., Iervolino, I., 2012. Spatial correlation of spectral acceleration in European data. *Bulletin of Seismological Society of America,* **102**(6):2781–2788.

Eurocode 8 Part 3, 2007. Design of structures for earthquake resistance-Assessment and retrofitting of buildings.

Falcucci, E., Gori, S., Galadini, F., Fubelli, G., Moro, M., Saroli, M., 2016. Active faults in the epicentral and mesoseismal Ml 6.0 24, 2016 Amatrice earthquake region, central Italy. *Method Seismotectonic Issues. Annals Geophys 59 Fast Track* **5**, 1-8.

Forte, G., Fabbrocino, S., Fabbrocino, G., Lanzano, G., Santucci de Magistris, F., Silvestri, F., 2017. A geolithological approach to seismic site classification: an application to the Molise Region (Italy). *Bulletin of Earthquake Engineering* **15**(1), 175-198.

Galadini, F., Galli, P., 2000. Active tectonics in the Central Apennines (Italy) - Input data for Seismic Hazard Assessment. *Natural Hazards*, **22**, 225-270.

Garcìa-Rodriguèz, M.J., Havenith, H.B., Benito, B., 2008. Evaluation of Earthquake- triggered landslides in El Salvador using a GIS based Newmark model. *14th Conference on Earthquake Engineering*, Beijing, China.

Goda, K., 2011. Interevent variability of spatial correlation of peak ground motions and response spectra. *Bulletin of Seismological Society of America,* **101**(5):2522–2531

Goda, K., Atkinson, G.M., 2010. Intraevent spatial correlation of ground-motion parameters using SK-net data. *Bulletin of Seismological Society of America* **100**(6):3055–3067

Grelle G., Bonito, L., Maresca, R., Maufroy, E., Revellino, P., Sappa, G., Guadagno, F., 2018. Topographic effects in Amatrice suggested from the SISERHMAP predictive model, seismic data and damage. *16th European Conference on Earthquake Engineering*, Thessaloniki, 18-21 June 2018.

Gru¨nthal, G., 1998. Cahiers du Centre Europe´en de Ge´odynamique et de Se´ismologie: volume 15—European Macroseismic Scale 1998. European Center for Geodynamics and Seismology, Luxembourg .

Jalayer F., Iervolino I., Manfredi G., 2010. Structural modeling uncertainties and their influence on seismic assessment of existing RC structures. *Structural Safety*, **32**(3), pp. 220-228.

Jalayer F., Ebrahimian H., 2017. Seismic risk assessment considering cumulative damage due to aftershocks. *Earthquake Engineering and Structural Dynamics*, **46**(3), 369-389.

Jalayer, F., Ebrahimian, H., Miano, A., Manfredi, G., Sezen, H., 2017. Analytical fragility assessment using un-scaled ground motion records. *Earthquake Engineering and Structural Dynamics*, **46**(15), 2639-2663.

Jayaram, N., Baker, J.W., 2009. Correlation model for spatially distributed ground-motion intensities. *Earthquake Engineering and Structural Dynamics*, **38**(15):1687–1708

Landolfi, L., Caccavale, M., d'Onofrio, A., Silvestri, F., Tropeano, G., 2011. Preliminary assessment of site stratigraphic amplification for Shakemap processing. *V International Conference on Earthquake Geotechnical Engineering*, Santiago, p.5.3.

Miano, A., Jalayer, F., De Risi, R., Prota, A., Manfredi, G., 2015. A case-study on scenario-based probabilistic seismic loss assessment for a portfolio of bridges. *12th international conference on applications of statistics and probability in civil engineering*, Vancouver, Canada, July 12–15, 2015.

Miano, A., Jalayer, F., De Risi, R., Prota, A., Manfredi, G., 2016. Model updating and seismic loss assessment for a portfolio of bridges. *Bulletin of Earthquake Engineering*, **14**(3): 699-719.

Miano, H. Sezen, F. Jalayer, A. Prota, Performance based comparison of different retrofit methods for reinforced concrete structures. *6th ECCOMAS Thematic Conference on Computational Methods in Structural Dynamics and Earth-quake Engineering (COMPDYN)*, Rhodes, Greece, 15-17 June 2017.

Miano, A., Jalayer, F., Ebrahimian, H., Prota, A., 2018. Cloud to IDA: Efficient fragility assessment with limited scaling. *Earthquake Engineering and Structural Dynamics*, **47**(5), 1124-1147.

Miano, A, Jalayer, F, Forte, G, Santo, A, 2019 (a). Vulnerability assessment for masonry buildings based on observed damage from the 2016 Amatrice Earthquake. *VII International Conference on Earthquake Geotechnical Engineering*, Rome, Italy, 17-20 June 2019.

Miano, A, Jalayer, F, Forte, G, Santo, A, 2019 (b). Empirical fragility assessment using conditional GMPE-based ground shaking fields: Application to damage data for 2016 Amatrice Earthquake. Bulletin of Earthquake Engineering, Submitted paper.

Michele, M, Di Stefano, R, …, Fares, M, 2016. The Amatrice 2016 seismic sequence: a preliminary look at the mainshock and aftershocks distribution. *Annals of Geophysics*, **59**, Fast Track 5, 1-8.

Park, J., Bazzurro, P., Baker, J.W., 2007. Modeling spatial correlation of ground motion intensity measures for regional seismic hazard and portfolio loss estimation. *Applications of statistics and probability in civil engineering*. Taylor & Francis Group, London, pp 1–8.

Polese, M., Gaetani d'Aragona, M., Prota, A., 2019. Simplified approach for building inventory and seismic damage assessment at the territorial scale: An application for a town in southern Italy. *Soil Dynamics and Earthquake Engineering*, **121**, 405-420.

Rota, M., Penna, A., Strobbia, C.L., 2008. Processing Italian damage data to derive typological fragility curves. *Soil Dynamics and Earthquake Engineering*, **28**(10-11), 933-947.

Silvestri, F., Forte, G., Calvello, M., 2016. Multi-level approach for zonation of seismic slope stability: Experiences and perspectives in Italy. *Landslides and Engineered Slopes. Experience, Theory and Practice –*

Aversa et al. (Eds) 2016 Associazione Geotecnica Italiana, Rome, Italy.

Singhal, A., Kiremidjian, A.S., 1998. Bayesian updating of fragilities with application to RC frames. *Journal of Structural Engineering*, **124**(8):922–929

Sokolov, V., Wenzel, F., 2011. Influence of spatial correlation of strong ground motion on uncertainty in earthquake loss estimation. *Earthquake Engineering and Structural Dynamics*, **40**(9):993–1009.

Tinti, E., Scognamiglio, L., Michelini, A., Cocco, M., 2016. Slip heterogeneity and directivity of the ML 6.0, 2016, Amatrice earthquake estimated with rapid finite-fault inversion. *Geophysical Research Letter*, **43**, 20 ,745-752.

Torgoev, A., Havenith, H.B., Lamair, L., 2013. Improvement of seismic landslide susceptibility assessment through consideration of geological and topographic amplification factors. *JAG 2013*, 17–18/09 Grenoble, France.

Tropeano, G., Soccodato, F.M., Silvestri, F., 2018. Re-evaluation of code-specified stratigraphic amplification factors based on Italian experimental records and numerical seismic response analyses. *Soil Dynamics and Earthquake Engineering*, **110**, 262-275.